Supporting Information

Synthesis of 2D MoO_{3-x}/N-doped-Carbon Nanocomposite via *in situ* Carbonization of Layered $(NH_4)Mo_3O_9$-$(NH_4)_2Mo_4O_{13}$-Organic Hybrid Nanomaterials for Exceptionally Efficient Adsorption and Separation of Organic Dye

Supriya Hanmant Gaikwad,[a, b] *and Shatabdi Porel Mukherjee**[a, b]

[a] Physical and Materials Chemistry Division, CSIR-National Chemical Laboratory (CSIR-NCL), Dr. Homi Bhabha Road, Pashan, Pune 411008, India,

[b] Academy of Scientific and Innovative Research (AcSIR), Ghaziabad-201002, India

Email: sp.mukherjee@ncl.res.in

Table of Contents

Table S3. Comparison of this work with previously reported literatures.

Figure S11. Zeta potential of MoO_{3-x}/N-C nanocomposite at various pH (1, ~7 and 9).

Figure S12. FT-IR spectra MoO_{3-x}/N-C nanocomposite, MB, MB adsorbed on MoO_{3-x}/N-C nanocomposite.

Figure S13. Schematic diagram of probable adsorption mechanism for MoO_{3-x}/N-C nanocomposite.

Figure S14: UV-vis spectra of a binary mixture composed with 50 ppm each of (a) MB and CV, (b) MB and MG, (c) MB and RhB solution before and after addition of MoO_{3-x}/N-C nanocomposite to equilibrate for 10-60 minutes in the dark; inset shows the color of the MB solution (i) before adsorption, (ii) after adsorbed by MoO_{3-x}/N-C nanocomposite, respectively for (a), (b) and (c).

Figure S15. XRD pattern of the MoO_{3-x}/N-C nanocomposite before and after corroded for 3 h using 2(M) HCl and 2(M) NaOH solution at pH 1 and pH 9 respectively.

References

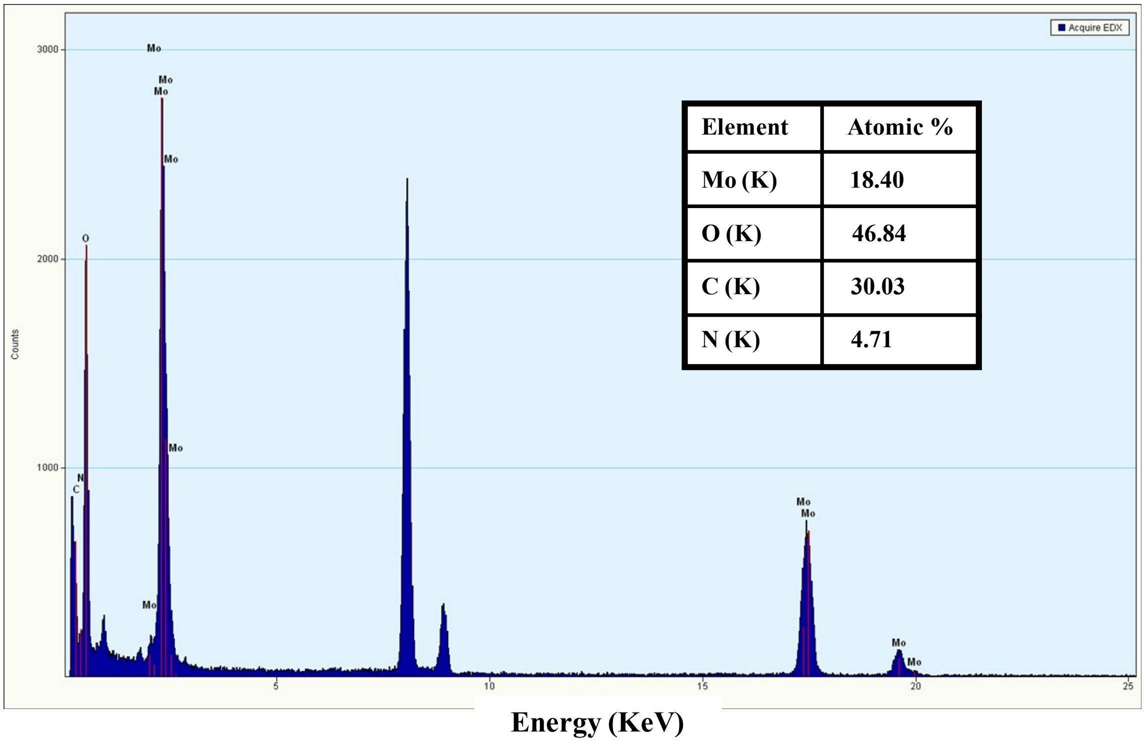

Element	Atomic %
Mo (K)	18.40
O (K)	46.84
C (K)	30.03
N (K)	4.71

Figure S1. TEM-EDS elemental analysis of MoO_{3-x}/N-C nanocomposite.

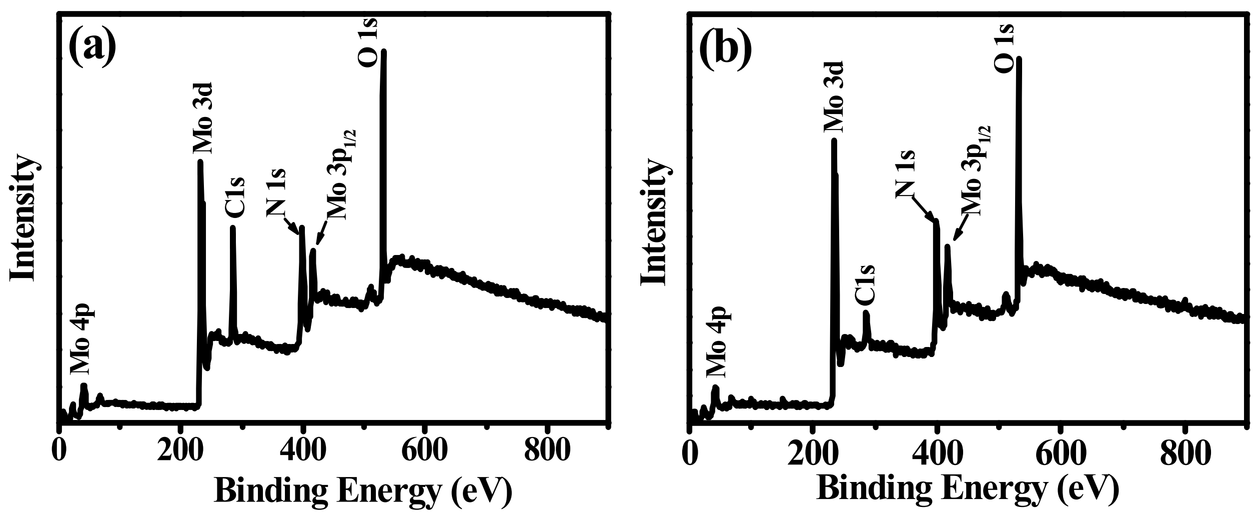

Figure S2. XPS survey spectra of (a) AMO-hybrid and (b) MoO_{3-x}/N-C nanocomposite.

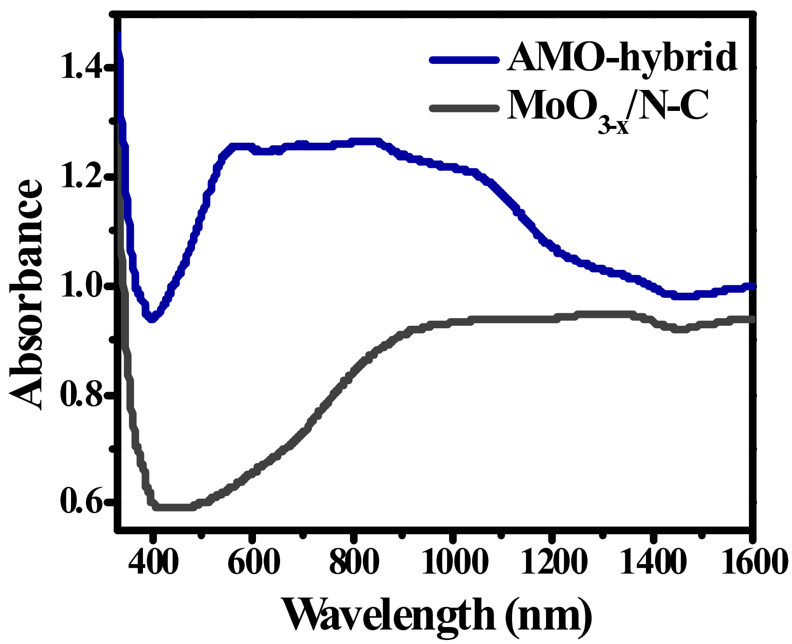

Figure S3. UV-vis-NIR diffuse reflectance spectra of AMO-hybrid and MoO_{3-x}/N-C nanocomposite.

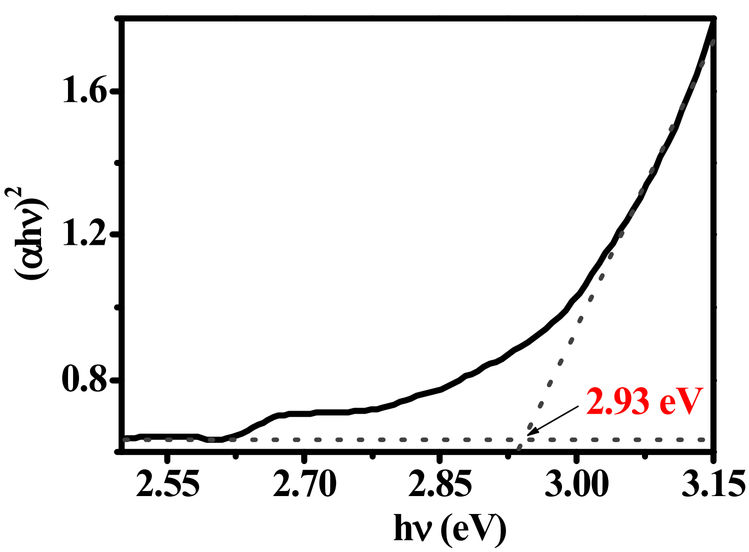

Figure S4. Typical 'Tauc' plots for calculating optical band gaps of MoO_{3-x}/N-C nanocomposite.

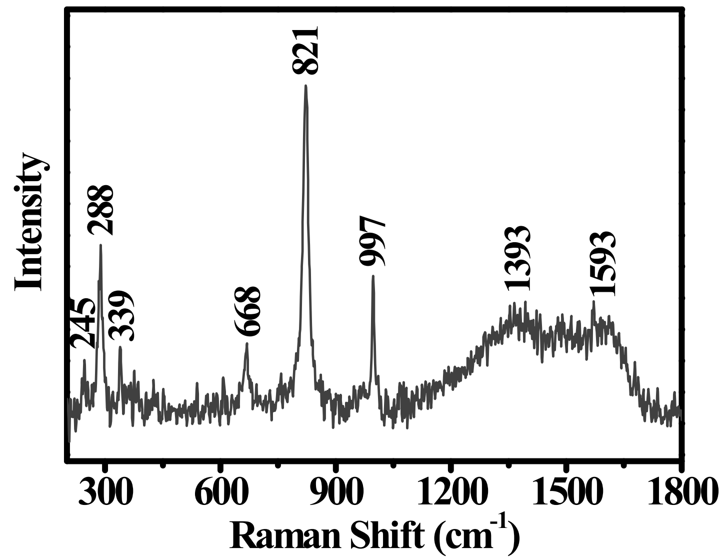

Figure S5. Raman spectra of MoO_{3-x}/N-C nanocomposite obtained at a laser power of 0.02 mW.

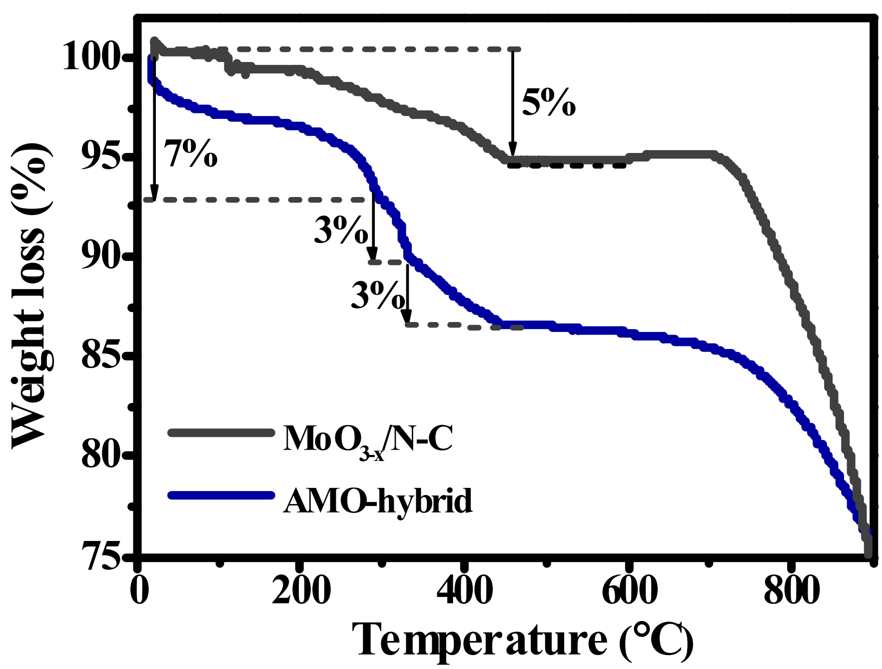

Figure S6. TGA analysis of AMO-hybrid and MoO_{3-x}/N-C nanocomposite.

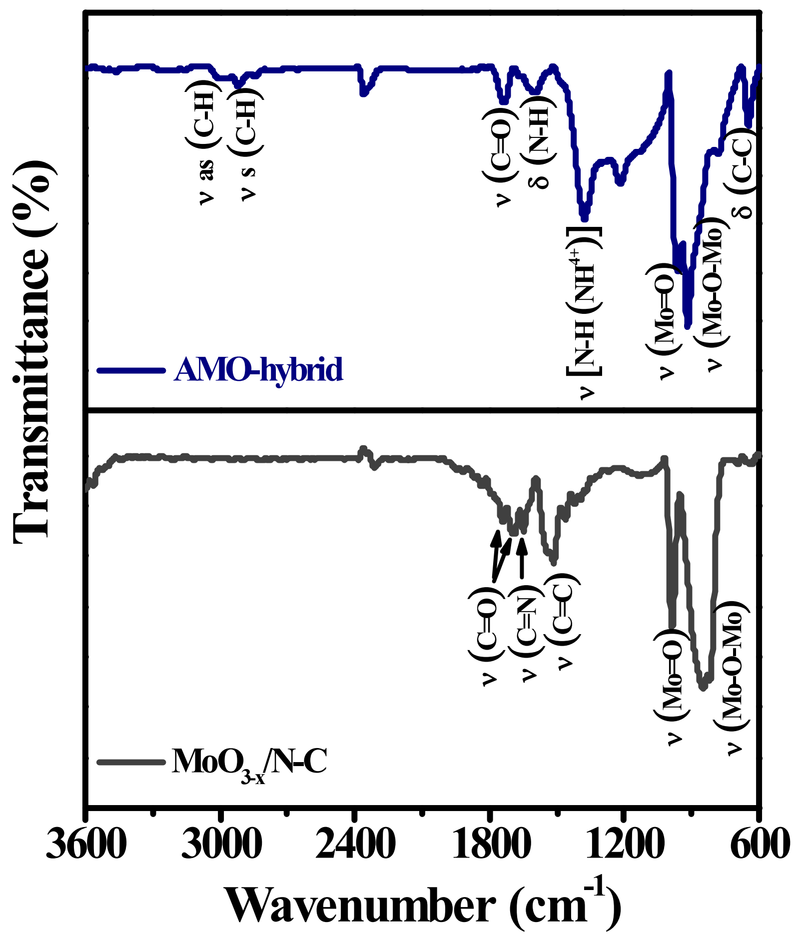

Figure S7. FT-IR spectra of samples; AMO-hybrid, MoO_{3-x}/N-C nanocomposite.*

* (ν = stretching vibration, ν_s = symmetric stretching vibration, ν_{as} = asymmetric stretching vibration, δ = bending vibration.)

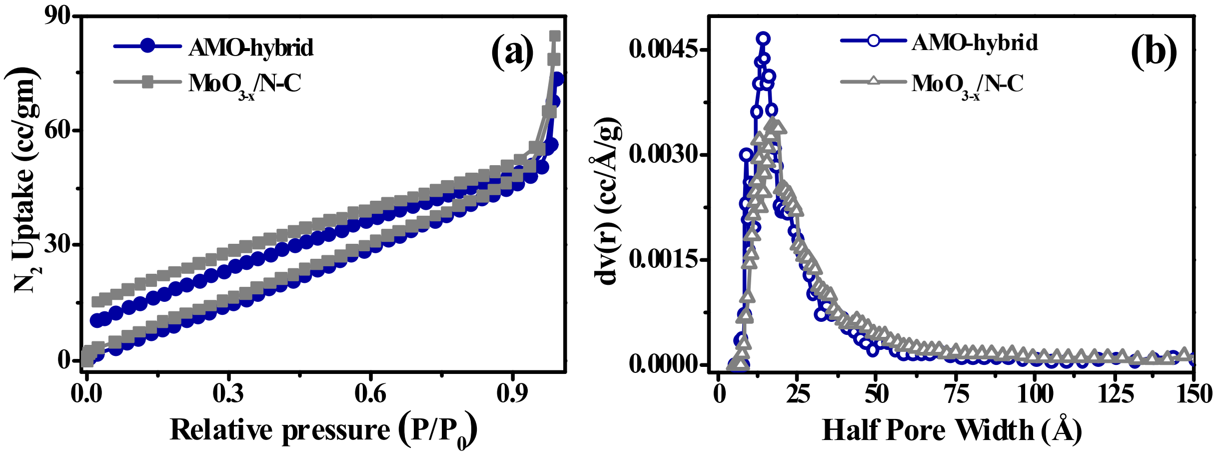

Figure S8. (a) N_2 adsorption/desorption isotherm and (b) pore size distribution calculated using DFT method slit pore model for AMO-hybrid and MoO_{3-x}/N-C nanocomposite.

Table S1. List of parameters deduced from nitrogen adsorption/desorption analysis of AMO-hybrid and MoO_{3-x}/N-C nanocomposite.

Sample	Surface Area (m^2/g)	Half pore width (Å)	Pore Volume (cc/g)
AMO-hybrid	80.895	13.84	0.078
MoO_{3-x}/N-C nanocomposite	69.897	17.16	0.090

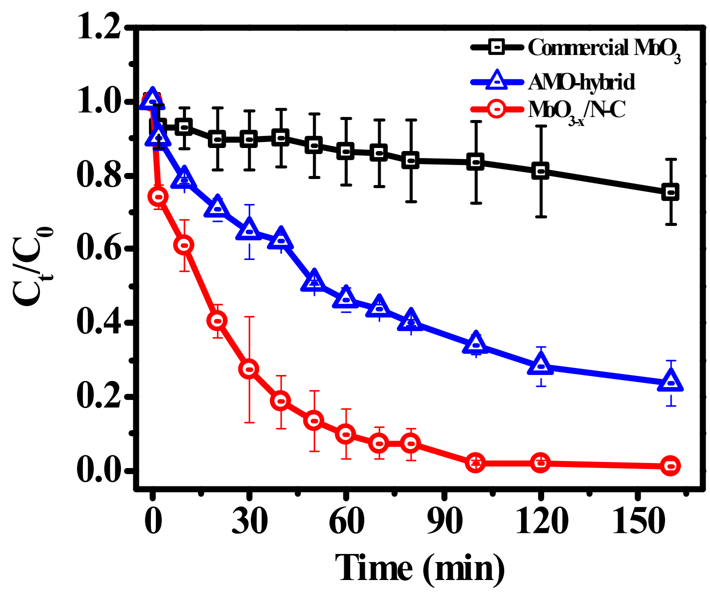

Figure S9. Comparison of adsorption capacity of as-synthesized MoO_{3-x}/N-C nanocomposite, AMO-hybrid and commercial MoO_3 on 100 ppm MB solution.*

*(C_0= 100 mg/L, M= 0.005 g, V= 0.005 L, T=160 min)

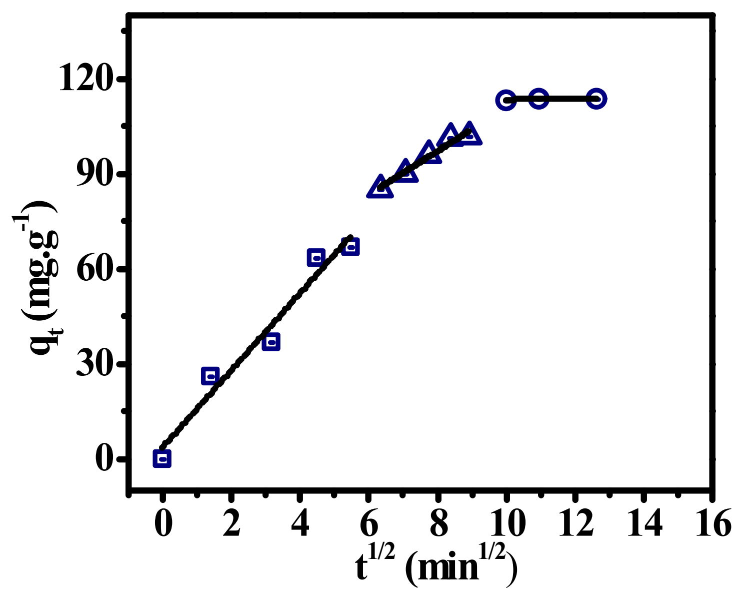

Figure S10. Adsorption kinetic plot of MB adsorbed on MoO_{3-x}/N-C nanocomposite fitted with intraparticle diffusion model.*

*(C_0= 100 mg/L, M= 0.005 g, V= 0.005 L, T=160 min)

Table S2. Adsorption kinetic parameters of MB adsorption onto MoO_{3-x}/N-C nanocomposite by nonlinear pseudo-first order, nonlinear pseudo-second order and intraparticle diffusion model.*

Models		Parameters	Values
Pseudo first order model		k_1	0.035
		$q_{e, exp}$ ($mg.g^{-1}$)	113.58
		$q_{e,cal1}$ ($mg.g^{-1}$)	112.18
		R^2	0.96
		χ^2	0.50
Pseudo second order model		k_2	0.00031
		$q_{e, exp}$ ($mg.g^{-1}$)	113.58
		$q_{e, cal2}$ ($mg.g^{-1}$)	134.31
		R^2	0.98
		χ^2	0.36
Intraparticle diffusion model	Stage 1	K_{di} ($mg.g^{-1}$ $min^{-0.5}$)	12.17
		C_i	3.17
		R^2	0.97
	Stage 2	K_{di} ($mg.g^{-1}$ $min^{-0.5}$)	8.86
		C_i	41.84
		R^2	0.96
	Stage 3	K_{di} ($mg.g^{-1}$ $min^{-0.5}$)	0.18
		Ci	111.34
		R^2	0.93

*$q_{e, cal}$ represent the calculated equilibrium adsorption capacity based on kinetic models, $q_{e, exp}$ is the experimental equilibrium adsorption capacity, K_{di} is the diffusion rate constant based on intraparticle diffusion (Weber-Morris) model.

Table S3. Comparison of this work with previously reported literatures.

Sr. No	Material	Surface area (m^2/g)	Adsorbate	Maximum adoption capacity Q_{max} (mg/g)	Time	pH	Recyclability		Selective adsorption/ separation, Separation efficiency (SE)	Reference
							Adsorption cycle, %	Desorption cycle, %		
1	MoO_{3-x} /N-C nanocomposite	70.97	MB	1360	72 h	Neutral	4, 99 %	4, 63-68 %	Selective adsorption towards cationic dyes (e.g., MB, RhB, SO CV, MG) Selective separation of MO from (i) Binary mixture (MB+MO) : SE = 99.77% (ii) Quaternary mixture (MB+CV+MG+MO) : SE = 75.68% (iii) Pentanary mixture (MB+SO+CV+MG+MO) : SE = 62.42%	This work
2	Mixed phase MoO_3 nanoparticles	5.17	MB	141.2	-	Neutral	-	-	-	1
3	h-MoO_3 rod-like microcrystals	-	MB	317.83	12h	6	4, 86%	-	-	2
4	MoO_3/MoO_2 composite nanoparticles	22.89	MB	1250	14 h	Neutral	4, 95%	-	-	3
5	MoO_{3-x} 3D nanoflower	-	MB RhB, MO	295.0	5 min	Neutral	3, 50%	-	Relatively higher adsorption towards RhB than MB and weak adsorption for MO from a	4

									ternary mixture containing MB, RhB, and MO	
6	MoO_3 nanospheres	-	MB	100% (20 ppm)	1 min	Neutral	-	-	-	5
7	α-MoO3 nanocrystals	42	MB	152	160 min	11	4 , 99%	-	-	6
8	MoO_3 nanoparticles	14	MB	98 % (20 ppm)	25 min	Neutral	-	-	-	7
9	α-MoO_3 flower like microsphere	17.7	RhB Methyl red, Alizarin yellow R	204.08	-	-	5, 98%	5, 70%	Selective adsorption towards RhB, methyl red, alizarin yellow R and no adsorption for MB, MO, fuchsin, cresol red, xylenol orange and alizarin red	8
10	α-MoO_3 flowers on carbon cloth	-	Rh B MB CV	4974* 6217* 3886* *(mg/m^2)	10 min	-	5, ~100%	-	-	9
11	α-MoO_3/ polyaniline composite	-	RhB Congo red	36.36 76.22	-	-	4, 82.1%	-	-	10
12	MoO_3 nanoparticle anchored in graphene	68	MB	625	-	Neutral	-	-	Selective adsorption towards MB and no adsorption for MO	11

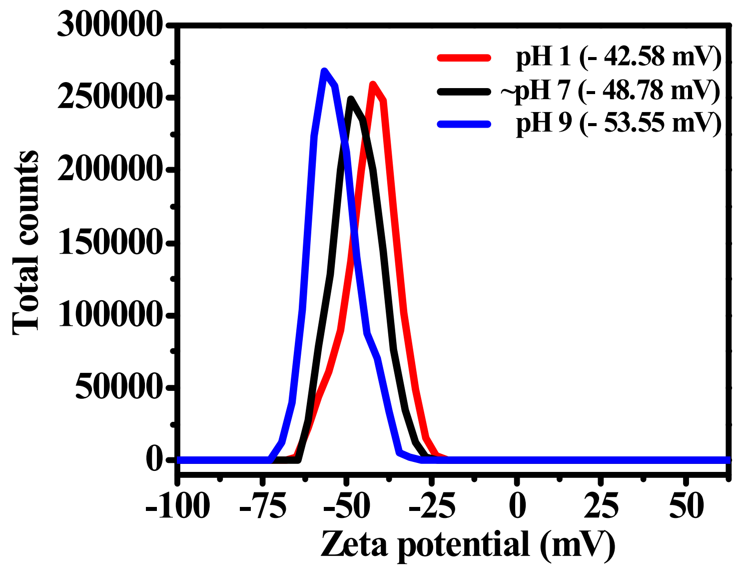

Figure S11. Zeta potential of MoO_{3-x}/N-C nanocomposite at various pH (1, ~7 and 9).

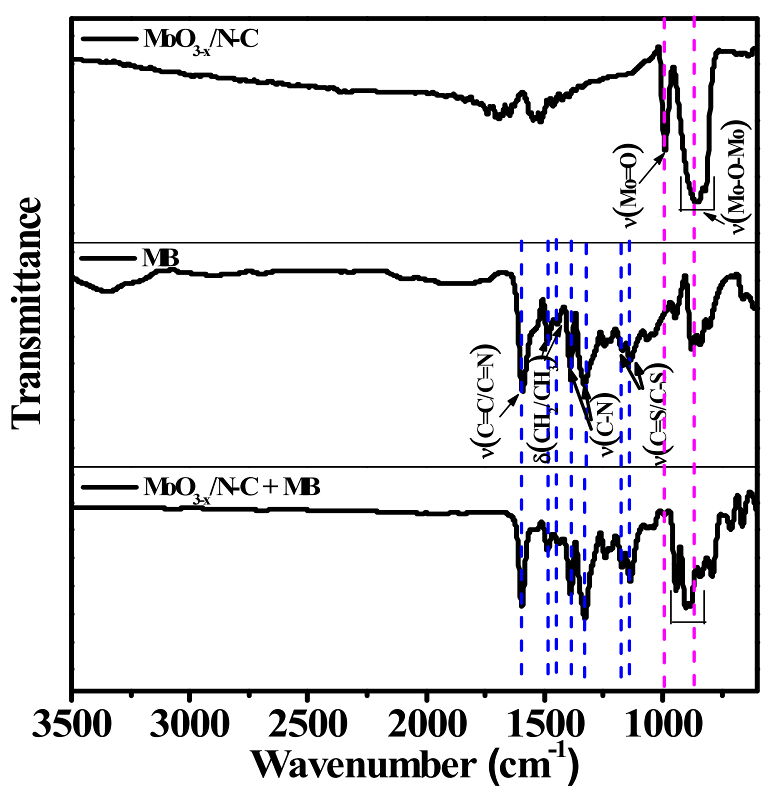

Figure S12. FT-IR spectra MoO_{3-x}/N-C nanocomposite, MB, MB adsorbed on MoO_{3-x}/N-C nanocomposite.

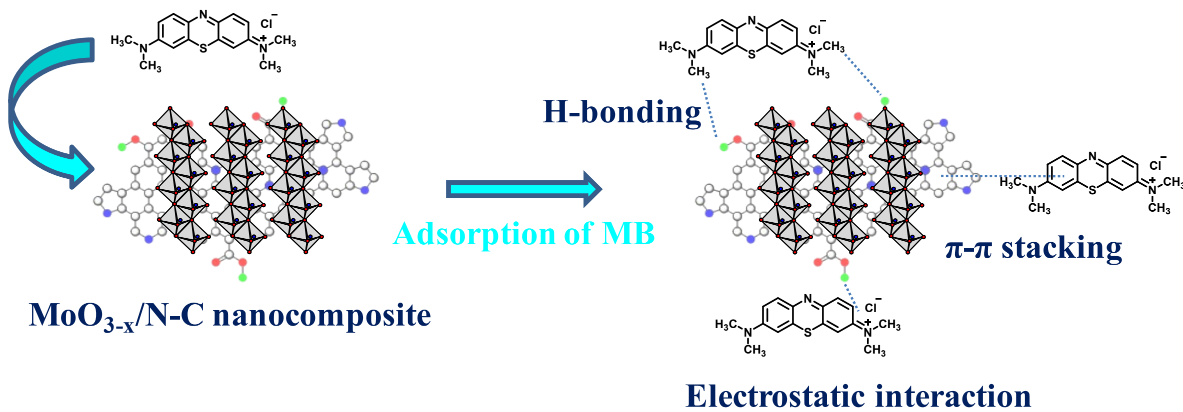

Figure S13. Schematic diagram of probable adsorption mechanism for MoO_{3-x}/N-C nanocomposite.

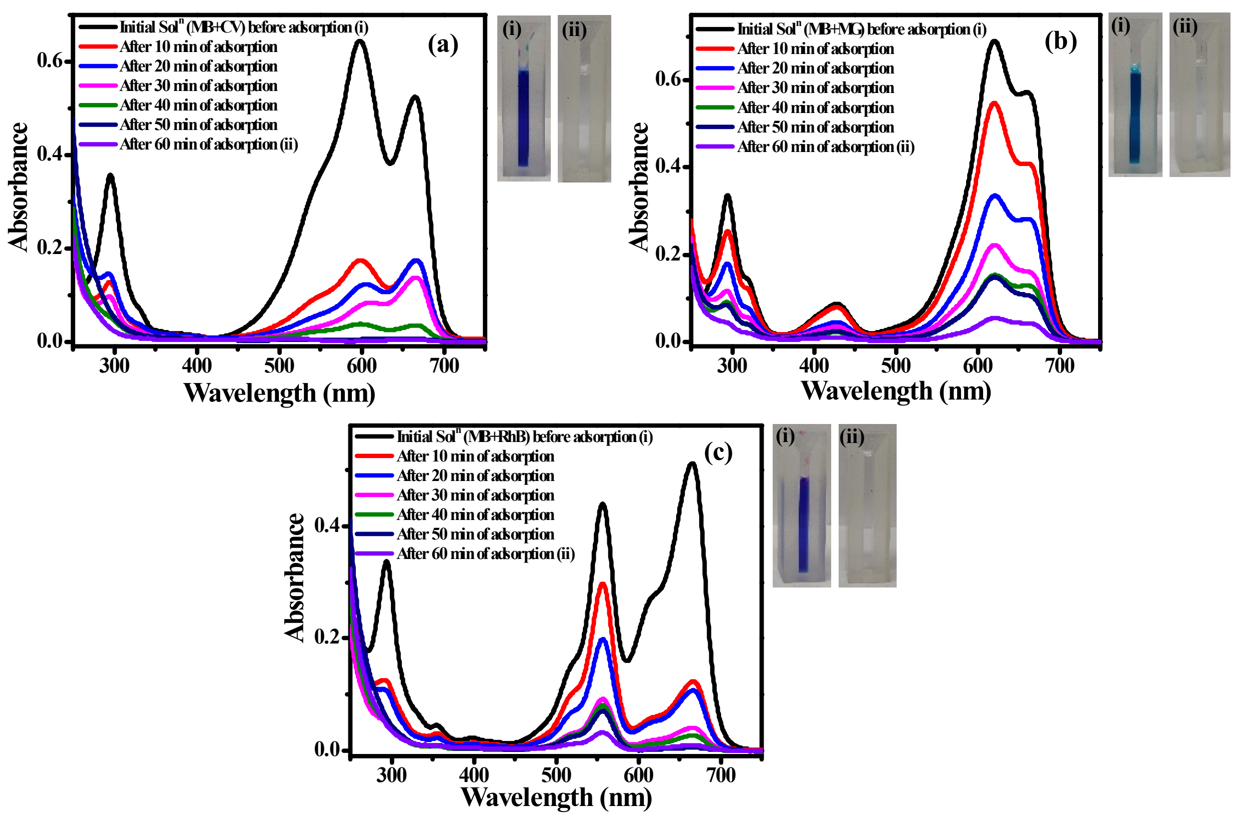

Figure S14: UV-vis spectra of a binary mixture composed with 50 ppm each of (a) MB and CV, (b) MB and MG, (c) MB and RhB solution before and after addition of MoO_{3-x}/N-C nanocomposite to equilibrate for 10-60 minutes in the dark; inset shows the color of the MB solution (i) before adsorption, (ii) after adsorbed by MoO_{3-x}/N-C nanocomposite, respectively for (a), (b) and (c).

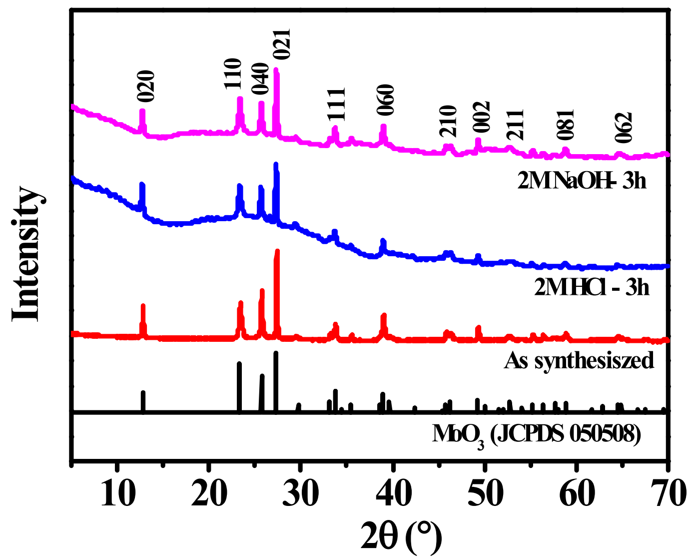

Figure S15. XRD pattern of the MoO_{3-x}/N-C nanocomposite before and after corroded for 3 h using 2(M) HCl and 2(M) NaOH solution at pH 1 and pH 9 respectively.

References

1. N. Kumar and R. Kumar, Efficient adsorption of methylene blue on hybrid structural phase of MoO_3 nanostructures, *Mater. Chem. Phys.,* 2022, **275***,* 125211.
2. M. L. de Sá, F. X. Nobre, L. d. S. Silva, G. d. S. Sousa, M. L. Takeno, E. A. J. Junior, J. M. E. d. M. Matos and M. R. M. C. d. Santos, Preparation of new *h*-MoO_3 rod-like microcrystals for effective removal of cationic dye in aqueous solution, *Int. J. Environ. Res*., 2021, **15***,* 105-124.
3. E. Taghipour and N. Tahmasebi, One-step hydrothermal synthesis of MoO_3/MoO_2 composite for efficient removal of methylene blue from aqueous solutions, *Mater. Today Commun.,* 2021, **26***,* 102012.
4. S. Huang, Y. Long, H. Yi, Z. Yang, L. Pang, Z. Jin, Q. Liao, L. Zhang, Y. Zhang, Y. Chen, H. Cui, J. Lu, X. Peng, H. Liang, S. Ruan and Y.-Z. Zeng, Multifunctional molybdenum oxide for solar-driven water evaporation and charged dyes adsorption, Appl. *Surf. Sci.,* 2019, **491**, 328-334.

5. D. Zhao, X. Zhang, H. Huan, X. Dong, H. Zhu, Z. Li, Y. Qi, J. Hu and X. Zeng, Facile synthesis of MoO_3 nanospheres and their application in water treatment, *Mater. Lett.*, 2019, **256**, 126648.

6. S. Rakass, H. Oudghiri Hassani, M. Abboudi, F. Kooli, A. Mohmoud, A. Aljuhani and F. Al Wadaani, Molybdenum Trioxide: Efficient Nanosorbent for Removal of Methylene Blue Dye from Aqueous Solutions, *Molecules,* 2018, **23**, 2295.

7. M. Santos-Beltra, F. Paraguay-Delgado, R. Garcıa, W. Antu´nez-Flores, C.Ornelas-Gutierrez and A. Santos-Beltra, Fast methylene blue removal by MoO_3 nanoparticles, *J. Mater. Sci. Mater. Electron.,* 2017, **28**, 2935-2948.

8. M. Wang, X.-X. Song, X.-L. Cheng, X. Zhou, X.-f. Zhang, Z. Cai, Y.-M.Xu, S.Gao, H. Zhao and L.-H. Huo, Highly selective and efficient adsorption dyes self-assembled by 3D hierarchical architecture of molybdenum oxide, *RSC Adv.,* 2015, **5**, 85248-85255.

9. D. Zhang, J. Li, J. Liang, H. Li and Y. Yan, Self-assembly of α-MoO_3 flower as a highly effective organics adsorbent for water purification, *J. Am. Ceram. Soc.*, 2019, **102**, 3307-3317.

10. S. Dhanavel, E. A. K. Nivethaa, K. Dhanapal, V. K. Gupta, V. Narayanan and A. Stephen, α-MoO_3/polyaniline composite for effective scavenging of rhodamine B, congo red and textile dye effluent, *RSC Adv.,* 2016, **6**, 28871-28886.

11. H. Lahan, R. Roy, N. D. Namsa and S. K. Das, MoO_3 nanoparticle anchored graphene as bifunctional agent for water purification, *Mater. Res. Express.,* 2016, **3**, 105003.